PHYSICAL REVIEW A VOLUME 23, NUMBER 5 MAY 1981

Incoherent-scattering cross sections in low- and medium-Z elements derived from the measured total attenuation cross sections in compounds

T. K. Umesh, C. Ranganathaiah, Ramakrishna Gowda, K. S. Puttaswamy, and B. Sanjeevaiah
Department of Physics, University of Mysore, Manasa Gangotri, Mysore 570006, India

(Received 9 July 1980; revised manuscript received 4 September 1980)

The whole-atom integral incoherent-scattering cross sections have been obtained from the total attenuation cross sections in elements whose atomic number (Z) ranges from 1 to 56, at photon energies 279.2, 514, 661.6, and 1115.5 keV. The total attenuation cross sections in elements were derived with the aid of mixture rule from total attenuation cross sections in 26 solid chemical compounds, measured by performing transmission experiments in a good geometry setup. The present values of the whole-atom integral incoherent-scattering cross sections have been compared with the Klein-Nishina cross sections, the self-consistent-field Hartree-Fock values of Hubbell *et al.*, and the available earlier experimental results. Electron binding effects have also been discussed.

INTRODUCTION

Among the various types of interactions of gamma rays with matter, the incoherent scattering is a dominant mode of interaction in the energy region 5 MeV down to a few keV. The incoherent scattering from free electrons is accurately described by the Klein-Nishina (KN) (Ref. 1) theory. Departures from the KN theory occur in situations where the incident gamma energies are comparable with the binding energies of the inner-shell electrons of the atom. The observed incoherent-scattering cross section σ_b can be expressed in terms of the KN cross section σ_{KN} as

$$\sigma_b = \sigma_{\mathrm{KN}} S(q, Z)\,, \qquad (1)$$

where $S(q,Z)$ is the incoherent-scattering function. Different models have been employed in order to calculate the incoherent-scattering function $S(q,z)$ whose magnitude is taken to be a measure of the electron binding. Of the various models in use, the Thomas-Fermi (TF) (Ref. 2) and the Hartree-Fock[3] (HF) are the most widely used. Grodstein[4] and Brown[5] have separately evaluated $S(q,z)$ by assuming the TF model for the atomic charge distribution. Storm and Israel[6] have employed the HF model in their evaluation of $S(q,z)$. More recently, the data of Hubbell *et al.*,[9] which make use of the self-consistent-field Hartree-Fock (SCF-HF) wave functions of Cromer,[7] Cromer and Mann,[8] have become available.

The experimental investigations on the incoherent scattering are relatively few. The experimental work done hitherto can be broadly classified into two categories: (1) determination of the whole-atom and shell-wise differential incoherent-scattering cross sections, and (2) determination of the whole-atom integral incoherent-scattering cross sections.

The differential incoherent-scattering cross-section measurements have been discussed in a recent paper by Shivaramu *et al.*[10] and the references cited therein.

In the determination of the whole-atom integral incoherent-scattering cross sections, the important measurements are of Ramana Rao *et al.*,[11] Gopal and Sanjeevaiah,[12] and Aruna Prasad *et al.*[13] In their investigation, the incoherent-scattering cross sections have been determined by subtracting the theoretical contributions due to other competing interactions from the experimental total attenuation cross sections of the elements, measured in a good geometry setup. Ramana Rao *et al.*[11] and Gopal and Sanjeevaiah[12] have observed deviations between experimental and theoretical values and have attributed them to the inadequacy of the incoherent-scattering functions. Aruna Prasad et al,[13] have reported good agreement of the experimental values of carbon, aluminum, and copper with the values based on the Hartree-Fock-Slater (HFS) model.

The recent values of Hubbell *et al.*[9] have not been tested adequately against experimental data. It can also be observed that the currently available experimental data on the whole-atom integral incoherent-scattering cross sections are deficient in the sense that very few elements have been covered. The data are scanty, particularly for elements which are not available abundantly in their solid elemental form. With a view to fill up the gaps in the currently available experimental data, 26 simple solid inorganic compounds which mostly contain low- and medium-Z ($Z = 1$ to 56) elements were selected and total attenuation cross sections were measured in a good geometry setup. The experimental values were used to derive the total attenuation cross sections of the constituent elements with the aid of the mixture rule.[14] The plot of the total attenuation cross sections versus atomic number is found to be linear in the low-Z region. This linearity can be attributed to the fact that in the present energy region the inco-

© 1981 The American Physical Society

herent-scattering cross section is dominant for low-Z elements. By making use of this linear portion of the plot, the whole-atom integral incoherent-scattering cross sections were derived. These values are compared with the SCF-HF values of Hubbell *et al.*[9] and with the available earlier experimental data.[11,12]

EXPERIMENTAL DETAILS

The geometrical setup used in the transmission experiment is similar to the one used in earlier experiments.[12,15] This setup satisfies the required good geometry conditions. However, in the present method, in place of the single-channel analyzer, a 1024-channel analyzer was used. The detector was a NaI(T1) crystal of dimension 1 in × 11/4 in, optically coupled to an RCA 6199 photomultiplier with a flat top along with a preamplifier. The preamplifier signal was then suitably amplified by a linear amplifier and the spectrum was recorded in a 1024-channel analyzer. The experiment was done in an air-conditioned room. The main voltage was stabilized. The drift in the amplifier gain was negligible.

Each chemical compound in fine-powder form was filled in cylindrical plastic containers. The mass of the compound was determined in an electrical balance correct to the third decimal place. The inner diameters of the plastic containers were determined with the help of a traveling microscope by the usual method. Using the values of the diameter and the mass of the compound, the mass per unit area was determined. A list of compounds used with their purities and molecular weights is given in Table I.

Monoenergetic gamma sources ^{203}Hg(279.2 keV), ^{85}Sr(514 keV), ^{137}Cs(661.6 keV), and ^{65}Zn(1115.5 keV) each of strength about 10 mCi, were obtained from the Bhabha Atomic Research Centre in the form of radiographic capsules. In the experiment, the empty plastic container was kept in the path of the beam and the unattenuated spectrum was recorded. The empty container was replaced by a container filled with the compound and the "attenuated" spectrum was recorded. In this way, the unattenuated spectrum and the attenuated spectrum were recorded alternately for all the compounds at all four energies. In the photopeak area of the attenuated spectra, five channels symmetrically located on either side of the centroid were selected and the counts due to all the eleven channels added. This gives the attenuated photon intensity I. The corresponding unattenuated intensity I_0 was determined in a

TABLE I. Purities and molecular weights of the compounds.

Sl No.	Compound	Molecular weight	Percentage purity	Manufacturers
1	LiOH	23.95	99.00	Sarabhai-Merck Pvt., Ltd.
2	MgO	40.31	99.00	E. Merck, Germany
3	NaF	41.99	99.00	Allied Chemicals, USA
4	NaCl	58.44	99.90	Sarabhai-Merck
5	$NaNO_2$	69.00	99.90	Sarabhai-Merck
6	KCl	74.56	99.80	British Drug Houses, Ltd.
7	NiO	74.71	99.00	Navrang Chemicals, Bombay
8	CuO	79.54	99.00	E. Merck, Germany
9	TiO_2	79.90	98.00	British Drug Houses, Ltd.
10	$NaHCO_3$	84.01	99.00	British Drug Houses, Ltd.
11	$NaNO_3$	85.00	98.00	May and Baker Pvt., Ltd.
12	MnO_2	86.94	98.00	E. Merck, Germany
13	CuCl	98.99	99.00	British Drug Houses
14	CrO_3	99.99	99.90	British Drug Houses
15	Al_2O_3	101.96	99.90	Reidel, West Germany
16	Na_2CO_3	105.99	99.50	E. Merck, Germany
17	KBr	119.02	99.00	British Drug Houses, Ltd.
18	RbCl	120.92	99.99	Riedel, Germany
19	ZrO_2	123.22	99.99	Riedel, Germany
20	SrF_2	125.62	99.99	Riedel, Germany
21	KH_2PO_4	136.09	99.70	British Drug Houses, Ltd.
22	Na_2SO_4	142.04	99.00	British Drug Houses, Ltd.
23	AgCl	143.32	98.00	E. Merck, Germany
24	BaO	153.34	99.00	British Drug Houses, Ltd.
25	KI	166.01	99.00	British Drug Houses, Ltd.
26	CdI_2	366.21	98.50	British Drug Houses, Ltd.

TABLE II. Total attenuation cross sections in compounds (barns/molecule). Figures in parentheses are the experimental errors.

Sl No.	Compound	279.2 keV	514 keV	661.6 keV	1115.5 keV
1	LiOH	4.33(0.05)	3.49(0.04)	3.11(0.04)	2.40(0.03)
2	MgO	7.24(0.15)	5.57(0.12)	5.18(0.10)	4.02(0.08)
3	NaF	7.18(0.12)	5.56(0.10)	5.15(0.09)	3.98(0.06)
4	NaCl	10.44(0.20)	7.81(0.16)	7.30(0.14)	5.62(0.08)
5	$NaNO_2$	12.19(0.12)	9.55(0.10)	8.76(0.09)	6.84(0.07)
6	KCl	13.68(0.15)	10.11(0.12)	9.60(0.11)	7.23(0.12)
7	NiO	14.54(0.29)	10.47(0.21)	9.56(0.20)	7.27(0.14)
8	CuO	15.19(0.30)	10.77(0.23)	9.78(0.22)	8.57(0.12)
9	TiO_2	14.28(0.30)	10.89(0.24)	9.98(0.23)	7.64(0.18)
10	$NaHCO_3$	15.03(0.12)	11.84(0.10)	10.83(0.09)	8.47(0.06)
11	$NaNO_3$	15.03(0.12)	11.82(0.10)	10.84(0.09)	8.46(0.07)
12	MnO_2	15.76(0.16)	11.74(0.12)	10.86(0.11)	8.28(0.08)
13	CuCl	18.79(0.27)	13.30(0.21)	12.20(0.21)	9.37(0.15)
14	CrO_3	18.02(0.36)	13.71(0.26)	12.64(0.15)	9.70(0.19)
15	Al_2O_3	17.88(0.18)	13.91(0.17)	12.94(0.16)	10.06(0.13)
16	Na_2CO_3	18.64(0.12)	14.53(0.10)	13.35(0.09)	10.47(0.06)
17	KBr	23.64(0.30)	16.07(0.21)	14.40(0.19)	10.96(0.15)
18	RbCl	24.54(0.44)	16.45(0.31)	14.42(0.28)	11.04(0.23)
19	ZrO_2	26.58(0.53)	17.49(0.37)	15.01(0.33)	11.53(0.26)
20	SrF_2	25.56(0.52)	17.22(0.36)	14.90(0.33)	11.36(0.26)
21	KH_2PO_4	24.94(0.27)	19.23(0.21)	17.88(0.19)	13.69(0.15)
22	Na_2SO_4	25.36(0.25)	19.60(0.20)	18.12(0.18)	14.10(0.14)
23	AgCl	36.94(0.78)	20.70(0.46)	17.80(0.41)	13.24(0.26)
24	BaO	50.44(0.96)	23.27(0.51)	19.86(0.42)	14.52(0.29)
25	KI	48.84(0.75)	24.31(0.46)	21.00(0.38)	15.43(0.25)
26	CdI_2	115.05(1.02)	54.40(0.66)	45.70(0.62)	33.34(0.50)

similar manner using the photopeak area of the unattenuated spectrum. The I's and I_0's determined in this way for all the compounds at all the four energies were then used to determine the total attenuation cross sections $\sigma_{\rm comp}$ using the relation

$$\sigma_{\rm comp} = \frac{A \ln(I_0/I)}{0.6025\,t} \qquad (2)$$

in units of barns/mol, where t is the mass per unit area in g/cm^2 and A is the gram molecular weight.

RESULTS AND DISCUSSION

The total attenuation cross sections thus obtained are tabulated in Table II along with experimental errors. The experimental errors are mainly due to (1) counting statistics, (2) multiple-scattering effects, (3) sample impurity, (4) nonuniformity in powder filling, (5) dead time of the counting instrument, and (6) pulse pileup effects.

The error due to counting statistics was kept below 0.3% by selecting the recording time such that about 10^5–10^6 counts were recorded at the photopeak, in all the cases.

The multiple scattering can result in several photons degraded in energy. There is a finite chance for these photons to be detected in the photopeak area, which results in an overestimation of the intensity I and hence an underestimation of $\sigma_{\rm comp}$. But, it was established using the extrapolation technique of Puttaswamy *et al.*[16] that the multiple-scattering effects were negligible in the present method.

The error due to sample impurity could be a significant factor only when large percentages of high-Z impurities are present in the sample. In the samples used, the content of high-Z impurities was less than 0.005%. The error due to sample impurity on the measured value of $\sigma_{\rm comp}$ was determined for all the compounds and it was found to be less than 1% at all the energies.

Nonuniformity in powder filling, if any, was checked by determining the intensity I by exposing different parts of the sample material to the incident beam. It was observed that any discrepancy in the intensity in each case was within counting statistics, which means that the error due to nonuniformity of powder is negligible. There is an in-built provision for dead-time correction in the 1024-channel analyzer. By keeping an optimal count rate the pulse pileup effects were kept to a minimum. Since monoenergetic sources were used it was felt that the detector resolution (8% for Cs^{137}) was sufficient for the purpose of the experiment. It may be argued that photon-dose build-up effects, as well as secondary effects like bremsstrahlung production, due to electrons which may be released in the sample could also contribute to the measured intensity. However, in view of the extremely low dosages used, the photon-dose build-up effects are considered to be negligible in this method. The photons released in the secondary interactions are of very low energy compared to that of the incident beam. Hence, the detector resolution is sufficient to resolve the two. Therefore, the counts due to secondary photons are recorded as background and do not contribute to the measured intensity I.

An error of about 1% arises from the small inaccuracy in the measurement of the mass per unit area of the samples. Corrections due to the short half-lives of ^{203}Hg and ^{85}Sr have also been incorporated. Thus, the overall errors on the measured values are less than 3%.

From these tabulated values, the attenuation cross sections for individual elements were derived using the mixture rule.[17] According to the mixture rule, the total attenuation cross section σ_{comp} of a compound system can be expressed in terms of the attenuation cross sections σ_i of its various atomic constituents, i.e.,

$$\sigma_{\text{comp}} = \sum_i n_i \sigma_i \,, \tag{3}$$

where n_i = number of atoms of the i^{th} element present in the compound (as indicated by the chemical formula for the compound).

The mixture rule ignores changes in the atomic wave functions, resulting from changes in the molecular, chemical, or crystalline environment of an atom. At very low energies (absorption edges), the errors from these approximations are

TABLE III. Total attenuation cross sections in elements (barns/atom). Figures in parentheses are the experimental errors.

	279.2 keV			514 keV		
Element	Present	Other experimental	Veigele	Present	Other experimental	Veigele
H	0.39(0.12)		0.36	0.32(0.10)		0.32
Li	1.10(0.05)		1.09	0.90(0.04)		0.86
C	2.12(0.12)	2.15(0.01)[b] 2.17(0.004)[a]	2.18	1.70(0.10)		1.69
N	2.51(0.12)		2.52	2.00(0.10)		2.02
O	2.84(0.12)		2.86	2.27(0.10)		2.27
F	3.18(0.12)		3.21	2.55(0.10)		2.57
Na	4.00(0.20)		4.05	3.01(0.16)		3.18
Mg	4.40(0.15)	4.40(0.02)[a]	4.38	3.30(0.12)		3.45
Al	4.68(0.18)	4.69(0.01)[b] 4.75(0.04)[c] 4.77(0.02)[a]	4.80	3.55(0.17)	3.60(0.04)[c]	3.73
P	5.56(0.27)		5.60	4.20(0.21)		4.31
S	6.00(0.25)	5.94(0.02)[a]	5.96	4.50(0.20)		4.64
Cl	6.44(0.27)		6.42	4.80(0.21)		4.90
K	7.24(0.15)		7.24	5.31(0.12)		5.59
Ti	8.60(0.30)	8.53(0.04)[a]	8.54	6.35(0.24)		6.46
Cr	9.50(0.36)		9.49	6.90(0.26)		7.03
Mn	10.08(0.16)		10.00	7.20(0.12)		7.40
Ni	11.70(0.29)	11.57(0.03)[a]	11.66	8.20(0.21)		8.33
Cu	12.35(0.30)	12.28(0.04)[b] 12.48(0.12)[c] 12.29(0.06)[a]	12.30	8.50(0.23)	8.59(0.09)[c]	8.65
Br	16.40(0.30)		16.61	10.76(0.21)		10.75
Rb	18.10(0.44)		18.42	11.65(0.31)		11.60
Sr	19.20(0.52)		19.50	12.12(0.36)		12.00
Zr	20.90(0.53)	21.08(0.14)[a] 21.20(0.20)[c]	21.10	12.95(0.37)	13.08(0.13)[c]	12.95
Ag	30.50(0.78)	30.40(0.09)[a] 31.00(0.30)[c]	31.00	15.90(0.46)	16.10(0.16)[c]	16.00
Cd	31.85(1.02)		32.00	16.40(0.66)		16.50
I	41.60(0.75)		41.00	19.00(0.46)		19.50
Ba	47.60(0.96)		47.50	21.00(0.51)		21.50

TABLE III. (*Continued*)

	661.6 keV				1115.5 keV	
Element	Present	Other experimental	Veigele	Present	Other experimental	Hubbell Ref. 22
H	0.28(0.09)	0.26(0.003) [d]	0.25	0.20(0.06)	0.20(0.002) [d]	0.20
Li	0.75(0.04)	0.76(0.01) [d]	0.76	0.58(0.03)	0.62(0.002) [d]	0.60
C	1.51(0.09)	1.54(0.01) [a] 1.54(0.01) [a] 1.54(0.01) [b]	1.51	1.21(0.06)	1.21(0.01) [a] 1.20(0.002) [d] 1.20(0.01) [b]	1.20
N	1.80(0.09)	1.82(0.02) [d]	1.79	1.40(0.07)	1.41(0.01) [d]	1.39
O	2.08(0.09)	2.07(0.03) [d]	2.03	1.62(0.07)	1.60(0.01) [d]	1.60
F	2.35(0.09)	2.34(0.03) [d]	2.30	1.78(0.06)	1.92(0.01) [d]	1.80
Na	2.80(0.14)	2.81(0.03) [d]	2.83	2.20(0.08)	2.18(0.01) [d]	2.20
Mg	3.10(0.10)	3.09(0.02) [a] 3.08(0.03) [d]	3.10	2.40(0.08)	2.41(0.01) [d] 2.43(0.01) [a]	2.42
Al	3.35(0.16)	3.33(0.01) [a] 3.40(0.03) [c] 3.33(0.06) [d] 3.33(0.01) [b]	3.35	2.60(0.13)	2.62(0.01) [b] 2.63(0.03) [c] 2.61(0.01) [d] 2.60(0.02) [a]	2.62
P	3.90(0.19)		3.84	3.00(0.15)		3.03
S	4.20(0.18)	4.17(0.02) [a] 4.17(0.03) [d]	4.22	3.22(0.14)	3.22(0.01) [d] 3.24(0.01) [a]	3.23
Cl	4.50(0.21)		4.42	3.42(0.15)		3.43
K	5.10(0.11)	4.99(0.05) [d]	5.10	3.81(0.12)	3.81(0.01) [d]	3.83
Ti	5.82(0.23)	5.67(0.02) [a] 5.70(0.10) [d]	5.84	4.40(0.18)	4.42(0.02) [d] 4.45(0.02) [a]	4.43
Cr	6.40(0.15)		6.34	4.84(0.19)		4.85
Mn	6.70(0.11)		6.58	5.04(0.08)		5.27
Ni	7.48(0.20)	7.31(0.03) [a]	7.38	5.65(0.14)	5.64(0.02) [a]	5.78
Cu	7.70(0.22)	7.69(0.04) [a] 7.68(0.02) [b] 7.78(0.08) [c]	7.70	5.95(0.12)	5.89(0.03) [b] 5.83(0.03) [a] 6.02(0.06) [c]	5.94
Br	9.30(0.19)	9.42(0.08) [d]	9.35	7.15(0.15)	7.15(0.01) [d]	7.19
Rb	9.92(0.28)	9.99(0.18) [d]	10.00	7.62(0.23)	7.58(0.04) [d]	7.61
Sr	10.20(0.33)		10.20	7.80(0.26)		7.85
Zr	10.85(0.33)	10.85(0.04) [a] 10.96(0.12) [c]	10.80	8.29(0.26)	8.17(0.03) [a] 8.38(0.09) [c] 8.19(0.04) [b]	8.24
Ag	13.30(0.41)	13.59(0.05) [a] 13.41(0.14) [c]	13.00	9.82(0.26)	9.94(0.04) [a] 9.92(0.10) [c]	9.97
Cd	13.90(0.62)		14.00	10.10(0.50)		10.19
I	15.90(0.38)	16.27(0.08) [d]	15.75	11.62(0.25)	11.44(0.02) [d]	11.69
Ba	17.78(0.42)	17.58(0.18) [d]	17.00	12.90(0.29)	12.22(0.05) [d]	12.50

[a] Conner *et al.*, Ref. 20.
[b] Gopal and Sanjeevaiah (Ref. 12).
[c] Values from measurements made with foils.
[d] Sinha and Chaudhuri (Ref. 19).

expected to be very large, while at higher energies, i.e., where the incident energy is very high compared to the absorption-edge energies, the mixture rule is believed to hold to a fairly good degree of accuracy.[18]

Most of the compounds used in the present measurements are either oxides or chlorides. Hence, the data on the total attenuation cross sections of oxygen and chlorine were obtained as follows: The difference between the experimental cross sections of sodium nitrate and sodium nitrite ($NaNO_3$ and $NaNO_2$) yields the cross sections for oxygen. These cross sections were used to extract the cross sections in copper from the experimental cross sections for the CuO (Cupric oxide) compound, and the cross sections obtained are in good agreement with the cross sections measured in 99.9% pure copper foils at the four photon energies of present interest. Further, the copper values were used to obtain the cross sections for chlorine from the CuCl (cuprous chloride) compound. These values of oxygen and

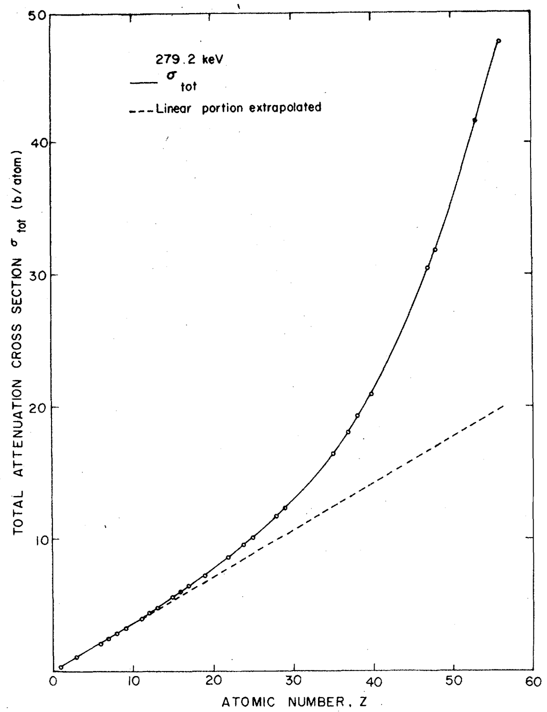

FIG. 1. Plot of derived total attenuation cross section against the atomic number of elements at 279.2 keV.

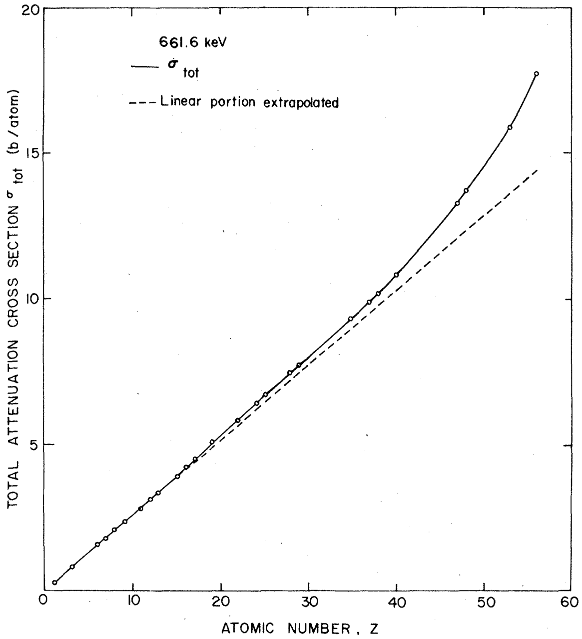

FIG. 3. Plot of derived total attenuation cross section against the atomic number of elements at 661.6 keV.

chlorine are used to derive the cross sections in other constituent elements. The derived cross sections are tabulated in Table III together with the measured values of Sinha and Chaudhuri,[19] Conner *et al.*,[20] and Gopal and Sanjeevaiah,[12] and also the interpolated values of Veigele[21] in case of 279.2, 514, and 661.6 keV and Hubbell *et al.*[22] for 1115.5 keV. The total attenuation cross sections were also measured in our setup using 99.9%-pure foils of Al, Cu, Zr, and Ag. These values have also been given in Table III for comparison. A good agreement between these values is observed. This indicates the reliability of the present method. A good agreement between the present values and the interpolated values is observed within the experimental errors. Further, derived

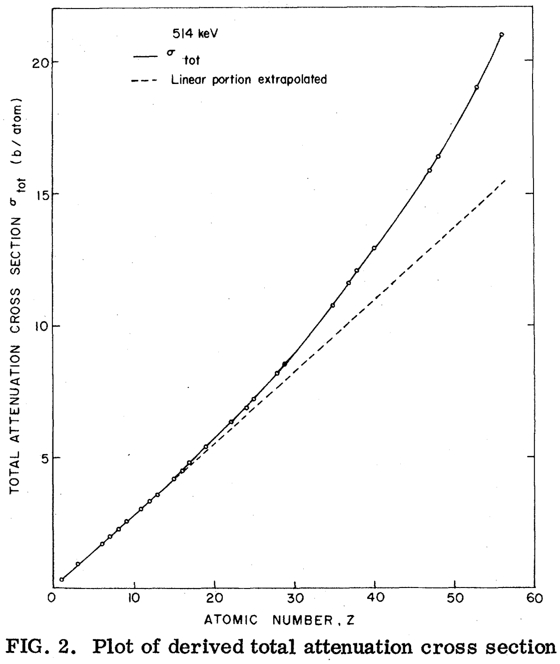

FIG. 2. Plot of derived total attenuation cross section against the atomic number of elements at 514 keV.

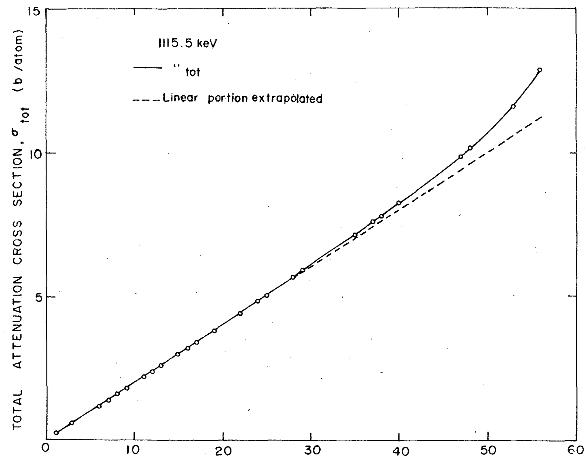

FIG. 4. Plot of derived total attenuation cross section against the atomic number of elements at 1115.5 keV.

total attenuation cross sections for the elements are plotted against the atomic number at each energy (Figs. 1–4). The plot is linear in the low-Z region. In the present energy region, the main mode of gamma-ray interaction with low-Z materials is the incoherent-scattering process. Hence, the initial linear portion of this plot can be strictly attributed to the incoherent-scattering cross sections only. For the initial linear portion, a straight line is fitted by the method of least squares. Using the fact that the incoherent-scattering cross sections vary linearly with the atomic number, this straight line is further extrapolated towards the region of higher Z. This yields the incoherent-scattering cross sections for the individual elements. These values are tabulated in Table IV along with the KN (Ref. 1) cross sections, the recent theoretical values of Hubbell *et al.*[9] and the available earlier experimental values.[11,12] The whole-atom integral incoherent-scattering cross sections were also obtained by subtracting the theoretical values of recent relativistic coherent-scattering cross sections[23] and the photoeffect cross sections,[24] from the present values of the derived total attenuation cross sections in individual elements. These values are also given in the same table for comparison.

From Table IV it is clear that there is a good agreement between the present values, the theoretical cross sections of Hubbell *et al.*,[9] and the available earlier experimental values.[11,12] The experimental errors on the total attenuation cross sections are directly carried over to the values of the incoherent-scattering cross sections. Therefore, the percentage error will be enhanced in the extrapolated region and will be up to 5%, except for hydrogen. In the case of hydrogen, an error as large as 30% creeps in because of the relatively larger contributions of elements Na, C, and O subtracted from the σ_{comp} of $NaHCO_3$ com-

TABLE IV. Whole-atom integral incoherent-scattering cross sections (barns/atom). Figures in parentheses are the experimental errors.

	279.2 keV				514 keV			
Element	Present	Subtraction values	KN Ref. 1	Hubbell Ref. 9	Present	Subtraction values	KN Ref. 1	Hubbell Ref. 9
H	0.37	0.37	0.36	0.37	0.33	0.32	0.29	0.29
Li	1.07	1.10	1.09	1.08	0.89	0.90	0.86	0.86
C	2.14	2.11	2.18	2.17	1.70	1.70	1.72	1.72
		2.12(0.02)^{b}						
		2.14(0.01)^{a}						
N	2.49	2.49	2.54	2.53	1.97	2.00	2.00	2.01
O	2.84	2.82	2.90	2.88	2.24	2.27	2.29	2.31
F	3.20	3.18	3.27	3.24	2.52	2.54	2.57	2.58
Na	3.90	3.93	3.99	3.96	3.06	3.00	3.14	3.15
Mg	4.26	4.29	4.35	4.32	3.34	3.28	3.43	3.43
Al	4.61	4.55	4.72	4.68	3.61	3.53	3.72	3.71
		4.55(0.05)^{b}						
		4.58(0.01)^{a}						
P	5.32	5.34	5.44	5.37	4.15	4.16	4.29	4.28
S	5.68	5.71	5.81	5.72	4.43	4.46	4.57	4.56
Cl	6.03	6.12	6.17	6.06	4.70	4.73	4.86	4.84
K	6.74	6.81	6.90	6.76	5.25	5.22	5.43	5.41
Ti	7.80	7.90	7.98	7.82	6.07	6.20	6.29	6.26
Cr	8.51	8.47	8.71	8.53	6.61	6.67	6.86	6.82
Mn	8.86	8.90	9.07	8.88	6.88	6.94	7.15	7.10
Ni	9.92	10.01	10.16	9.94	7.70	7.81	8.01	7.94
Cu	10.28	10.33	10.52	10.29	7.98	8.05	8.29	8.22
		9.80(0.10)^{b}						
		10.04(0.04)^{a}						
Br	12.40	12.04	12.70	12.41	9.61	9.86	10.01	9.91
Rb	13.11	12.50	13.43	13.11	10.16	10.50	10.58	10.46
Sr	13.46	13.28	13.79	13.46	10.43	10.86	10.86	10.74
Zr	14.17	13.75	14.52	14.16	10.98	11.37	11.44	11.31
Ag	16.65	15.70	17.06	16.63	12.89	13.00	13.44	13.27
Cd	17.00	{16.35 15.70(0.40)^{b}	17.42	16.98	13.16	13.27	13.72	13.55
I	18.77	19.05	19.23	18.74	14.53	14.20	15.15	14.96
Ba	19.84	19.38	20.32	19.79	15.35	14.84	16.01	15.80

TABLE IV. (*Continued.*)

		661.6 keV				1115.5 keV		
Element	Present	Subtraction values	KN Ref. 1	Hubbell Ref. 9	Present	Subtraction values	KN Ref. 1	Hubbell Ref. 9
H	0.28	0.28	0.26	0.26	0.19	0.20	0.20	0.20
Li	0.77	0.75	0.77	0.77	0.59	0.58	0.60	0.61
C	1.55	1.51 1.54(0.01)[a]	1.54	1.54	1.20	1.21	1.20	1.21
N	1.80	1.80	1.79	1.80	1.40	1.40	1.40	1.41
O	2.06	2.08	2.05	2.06	1.60	1.62	1.60	1.61
F	2.32	2.35	2.31	2.31	1.80	1.78	1.80	1.81
Na	2.84	2.79	2.82	2.82	2.20	2.20	2.20	2.21
Mg	3.09	3.09	3.07	3.08	2.40	2.40	2.40	2.42
Al	3.35	3.34 3.32(0.01)[a]	3.33	3.34	2.60	2.59	2.60	2.62
P	3.87	3.87	3.84	3.86	3.01	2.99	3.00	3.02
S	4.13	4.17	4.10	4.12	3.21	3.21	3.20	3.22
Cl	4.38	4.46	4.36	4.38	3.41	3.41	3.40	3.42
K	4.90	5.04	4.61	4.89	3.81	3.78	3.80	3.82
Ti	5.67	5.74	5.64	5.65	4.41	4.35	4.40	4.42
Cr	6.19	6.27	6.15	6.16	4.81	4.79	4.80	4.81
Mn	6.45	6.56	6.41	6.40	5.02	4.97	5.00	5.02
Ni	7.22	7.27	7.17	7.17	5.62	5.55	5.60	5.61
Cu	7.48	7.45 7.44(0.02)[a]	7.43	7.42	5.82	5.85	5.80	5.81
Br	9.03	8.78	8.97	8.95	7.03	6.96	7.00	7.01
Rb	9.54	9.29	9.48	9.45	7.43	7.41	7.40	7.41
Sr	9.80	9.49	9.74	9.70	7.63	7.55	7.60	7.61
Zr	10.32	9.98	10.25	10.21	8.03	8.00	8.00	8.00
Ag	12.12	11.48	12.04	11.98	9.44	9.15	9.40	9.40
Cd	12.38	11.85	12.30	12.23	9.64	9.36	9.60	9.60
I	13.67	13.26	13.58	13.50	10.64	10.57	10.61	10.60
Ba	14.45	14.41	14.35	14.26	11.25	11.60	11.21	11.20

[a] Gopal and Sanjeevaiah (Ref. 12).
[b] Ramana Rao *et al.* (Ref. 11).

pound. From Table IV it is also evident that the deviations between the bound-electron cross sections (present values) and the free-electron cross sections (KN values) increase as Z increases at 279.2 and 514 keV. This indicates that the electron binding effects increase as Z increases for a given energy. At higher energies, binding effects show up only above $Z = 40$.

ACKNOWLEDGMENT

One of the authors (T.K.U) would like to thank the Council of Scientific and Industrial Research (India) for awarding him a Junior Research Fellowship.

---

[1] O. Klein and Y. Nishina, Z. Phys. 52, 853 (1929).

[2] L. H. Thomas, Proc. Cambridge Philos. Soc. 23, 542 (1926); E. Fermi, Z. Phys. 48, 73 (1928).

[3] Fock, Z. Phys. 61, 126 (1930); D. R. Hartree, Proc. Cambridge Philos. Soc. 24, 89 (1928).

[4] G. Grodstein, NBS Circular No. 583, 1957 (unpublished).

[5] W. D. Brown, Boeing Company Reports Nos. D2-125136-1, 1966 and D2-125137-1, 1966 (unpublished).

[6] I. Storm and E. Israel, Nucl. Data Tables A1, 565 (1970).

[7] D. T. Cromer, J. Chem. Phys. 50, 4857 (1969).

[8] D. T. Cromer and J. B. Mann, J. Chem. Phys. 47, 1892 (1967).

[9] J. H. Hubbell, Wm. J. Veigele, E. A. Briggs, R. T. Brown, D. T. Cromer, and R. J. Howerton, J. Phys. Chem. Ref. Data 4, 471 (1975).

[10] Shivaramu, S. Gopal, and B. Sanjeevaiah, J. Phys. B 13, 273 (1980).

[11] P. V. Ramana Rao, J. Rama Rao, and V. Lakshminarayana, Proc. Phys. Soc. London 85, 1081 (1965); 39, 195 (1965); Indian J. Pure Appl. Phys. 4, 56 (1966).

[12] S. Gopal and B. Sanjeevaiah, Nucl. Instrum. Methods 107, 221 (1973); J. Phys. B 6, 2441 (1973); Phys. Rev.

A 8, 2814 (1973); Ph.D. thesis, 1973, Mysore University (unpublished).

[13] G. Aruna Prasad, K. Parthasaradhi, and V. Lakshminarayana, J. Mysore University B26, 121 (1976-77).

[14] R. D. Deslattes, AFOSR Report No. TN-58-784, 1958 (unpublished); Acta Crystallogr. A35, 89 (1969).

[15] Ramakrishna Gowda and B. Sanjeevaiah, Phys. Rev. A 9, 2569 (1974).

[16] K. S. Puttaswamy, Ramakrishna Gowda, and B. Sanjeevaiah, Can. J. Phys. 57, 92 (1979).

[17] R. H. Millar and J. R. Greening, J. Phys. B 7, 2332 (1974).

[18] J. H. Hubbell, Nat. Stand. Ref. Data Ser. Nat. Bur. Stand. 29, (1969).

[19] B. Sinha (Goswami) and N. Chadhuri, Phys. Rev. A 7, 1912 (1973).

[20] A. L. Conner, H. F. Atwater, E. H. Plassman, and J. H. McCrary Phys. Rev. A 1, 539 (1970).

[21] William, J. Veigele, Atomic Data Tables 5, 51 (1973).

[22] J. H. Hubbell, H. A. Gimm, and I. Overbø (private communication); J. Phys. Chem. Ref. Data (in press).

[23] J. H. Hubbell and J. Overbø, J. Phys. Chem. Ref. Data 8, 69 (1979).

[24] J. H. Scofield, UCRL Report No. 51326, 1973 (unpublished).